Research Article | Vol. 26, No. 2 | 22 Jan 2018 | OPTICS EXPRESS 990
Optics EXPRESS

Time-bandwidth compression of microwave signals

MING LI,[1,2*] SHUQIAN SUN,[1,2] BO LI,[3] HOSSEIN ASGHARI,[4] YE DENG,[1,2] WEI LI[1,2] AND NINGHUA ZHU[1,2]

[1]*State Key Laboratory on Integrated Optoelectronics, Institute of Semiconductors, Chinese Academy of Sciences, Beijing 100083, China*
[2]*School of Electronic, Electrical and Communication Engineering, University of Chinese Academy of Science, Beijing 100049, China*
[3]*Institut National de la Recherche Scientifique-Energie, Materiaux et Telecommunications, Montreal, Quebec H5A 1K6, Canada*
[4]*Department of Electrical Engineering and Computer Science, Loyola Marymount University, Los Angeles, California 900945, USA*
[*]*ml@semi.ac.cn*

Abstract: We report and demonstrate a reconfigurable photonic anamorphic stretch transform to realize time-bandwidth product (TBP) compression for microwave signals. A time-spectrum convolution system is employed to provide an ultra-high nonlinear dispersion up to several nanoseconds per gigahertz, which is required for processing nanosecond-long microwave signals. The group delay of the system can be engineered easily by programming a WaveShaper. Based on the proposed scheme, the TBP of a double pulse microwave signal is compressed by 1.9 times. Our proposal can provide a more efficient way to sample, digitize and store high-speed microwave signals, opening up entirely new perspectives for generation of many critical microwave signal processing modules.

OCIS codes: (070.1170) Analog optical signal processing; (120.0120) Instrumentation, measurement, and metrology; (260.2030) Dispersion; (350.4010) Microwaves.

References and links

1. A. S. Bhushan, F. Coppinger, and B. Jalali, "Time-stretche danalogue-to-digital conversion," Electron. Lett. **34**(9), 839–841 (1998).
2. F. Coppinger, A. S. Bhushan, and B. Jalali, "Time magnification of electrical signals using chirped optical pulses," Electron. Lett. **34**(4), 399–400 (1998).
3. A. M. Fard, S. Gupta, and B. Jalali, "Photonic time-stretch digitizer and its extension to real-time spectroscopy and imaging," Laser Photonics Rev. **7**(2), 207–263 (2013).
4. D. R. Solli, C. Ropers, P. Koonath, and B. Jalali, "Optical rogue waves," Nature **450**(7172), 1054–1057 (2007).
5. F. Qian, Q. Song, E. Tien, S. K. Kalyoncu, and O. Boyraz, "Real-time optical imaging and tracking of micron-sized particles," Opt. Commun. **282**(24), 4672–4675 (2009).
6. C. Zhang, Y. Qiu, R. Zhu, K. K. Y. Wong, and K. K. Tsia, "Serial time-encoded amplified microscopy (STEAM) based on a stabilized picosecond supercontinuum source," Opt. Express **19**(17), 15810–15816 (2011).
7. F. Xing, H. Chen, M. Chen, S. Yang, and S. Xie, "Simple approach for fast real-time line scan microscopic imaging," Appl. Opt. **52**(28), 7049–7053 (2013).
8. K. Goda, K. K. Tsia, and B. Jalali, "Amplified dispersive fourier-transform imaging for ultrafast displacement sensing and barcode reading," Appl. Phys. Lett. **93**(13), 131109 (2008).
9. Y. Deng, M. Li, N. Huang, J. Azaña, and N. Zhu, "Serial time-encoded amplified microscopy for ultrafast imaging based on multi-wavelength laser," Chin. Sci. Bull. **59**(22), 2693–2701 (2014).
10. T. T. W. Wong, A. K. S. Lau, K. K. Y. Ho, M. Y. H. Tang, J. D. F. Robles, X. Wei, A. C. S. Chan, A. H. L. Tang, E. Y. Lam, K. K. Y. Wong, G. C. F. Chan, H. C. Shum, and K. K. Tsia, "Asymmetric-detection time-stretch optical microscopy (ATOM) for ultrafast high-contrast cellular imaging in flow," Sci. Rep. **4**(1), 3656 (2015).
11. G. C. Valley, "Photonic analog-to-digital converters," Opt. Express **15**(5), 1955–1982 (2007).
12. J. Stigwall and S. Galt, "Signal reconstruction by phase retrieval and optical backpropagation in phase-diverse photonic time-stretch systems," J. Lightwave Technol. **25**(10), 3017–3027 (2007).
13. W. Ng, T. D. Rockwood, G. A. Sefler, and G. C. Valley, "Demonstration of a large stretch-ratio (m=41) photonic analog-to-digital converter with 8 enob for an input signal bandwidth of 10 ghz," IEEE Photon. Technol. Lett. **24**(14), 1185–1187 (2012).

#309067 https://doi.org/10.1364/OE.26.000990
Journal © 2018 Received 12 Oct 2017; revised 17 Dec 2017; accepted 21 Dec 2017; published 10 Jan 2018

Optics EXPRESS

14. Y. Han, O. Boyraz, and B. Jalali, "Ultrawide-band photonic time-stretch a/d converter employing phase diversity," IEEE Trans. Microw.Theory **53**(4), 1404–1408 (2005).
15. J. Fuster, D. Novak, A. Nirmalathas, and J. Marti, "Singlesideband modulation in photonic time-stretch analogue-todigital conversion," Electron. Lett. **37**(1), 67–68 (2001).
16. J. Chou, O. Boyraz, D. Solli, and B. Jalali, "Femtosecond real-time single-shot digitizer," Appl. Phys. Lett. **91**(16), 161105 (2007).
17. K. Goda, K. K. Tsia, and B. Jalali, "Serial time-encoded amplified imaging for real-time observation of fast dynamic phenomena," Nature **458**(7242), 1145–1149 (2009).
18. K. K. Tsia, K. Goda, D. Capewell, and B. Jalali, "Performance of serial time-encoded amplified microscope," Opt. Express **18**(10), 10016–10028 (2010).
19. M. H. Asghari and B. Jalali, "Experimental demonstration of optical real-time data compressiona)," Appl. Phys. Lett. **104**(11), 111101 (2014).
20. M. H. Asghari and B. Jalali, "Anamorphic transformation and its application to time-bandwidth compression," Appl. Opt. **52**(27), 6735–6743 (2013).
21. B. Jalali, J. Chan, and M. H. Asghari, "Time-bandwidth engineering," Optica **1**(1), 23–31 (2014).
22. B. Jalali and A. Mahjoubfar, "Tailoring wideband signals with a photonic hardware accelerator," Proc. IEEE **103**(7), 1071–1086 (2015).
23. Y. Park and J. Azaña, "Ultrahigh dispersion of broadband microwave signals by incoherent photonic processing," Opt. Express **18**(14), 14752–14761 (2010).
24. A. Mahjoubfar, C. L. Chen, and B. Jalali, "Design of warped stretch transform," Sci. Rep. **5**(1), 17148 (2015).
25. B. Li and J. Azaña, "Incoherent-light temporal stretching of high-speed intensity waveforms," Opt. Lett. **39**(14), 4243–4246 (2014).

1. Introduction

Data capacity has been growing explosively with the rapid development of mobile internet and sensor technology along with wireless sensing networks. As a result, the analysis, measurement, storage and transmission of such huge amounts of data have been recognized as an important and urgent issues for the development of modern information techniques. However, there are two limiting issues to acquire, compress or digitize increasingly dynamic and fast information flow: 1) the sampling rate of conventional information processing techniques is supposed to be at least two times larger than the signal bandwidth, which is referred to as Nyquist's Theorem; 2) for dynamic signals, the signal with a bandwidth lower than Nyquist frequency will be oversampled, leading to a waste of system cost.

The bandwidth and sampling rate of analog-to-digital converters is the main bottleneck in real-time acquisition and processing of fast waveforms. The photonic time-stretch technology provides a unique and practical solution to this problem and has been widely applied in ultrafast optical spectrum analysis [1–4], imaging [5–10] and broadband analog-to-digital conversion [1–3,11–18]. Photonic time-stretch transform is a technique that temporally stretches the fast signal based on linear photonic dispersion delay lines so that the bandwidth of the signal will be compressed by a factor M [15–19]. However, the record time of the stretched signal increases with the same factor M (see Fig. 1). In other words, the time-bandwidth product (TBP) of signal remains unchanged. Therefore, dynamic signals with bandwidth lower than the Nyquist frequency are still oversampled. To solve this problem, anamorphic stretch transform (AST), a type of warped stretch transform, capable of TBP compression has been proposed (see Fig. 1). This technique replaces linear dispersive devices with an engineered nonlinear dispersive device [19–21]. The problem of insufficient sampling rate is solved, and simultaneously the time-bandwidth product of the stretched signal is compressed, leading to a shorter record length for the same bandwidth. Arbitrary stretch profiles and time bandwidth product can be synthesized using nonlinear dispersion primitives and stretch basis functions [21]. Reconstruction of the warped waveform requires information about the phase which can be obtained via coherent detection or phase retrieval techniques [22].

In many applications such as laser imaging, radar imaging and high-speed photography, the signal bandwidths are typically from several GHz to several tens of gigahertz. Whereas a time-stretch transform based on optical dispersive devices usually offer dispersion values much less than 1ns/GHz. These optical dispersive lines are unable to meet the requirement of

Optics EXPRESS

stretching nanosecond-long microwave signals. Additionally, a nonlinear optical dispersive device [19] (e.g. chirped fiber Bragg grating) is usually designed to produce a specific group delay profile with no or limited reconfigurability. A more flexible approach would be to design a programmable dispersive line which can provide tunable group delay profiles.

In this article, we propose and realize a microwave AST system with ultra-high nonlinear dispersion and reconfigurable group delay profiles. The proposed scheme is implemented based on a time-spectrum convolution (TSC) system [23], providing a microwave dispersion up to several nanoseconds per gigahertz. The group delay profiles could be engineered easily by programming the WaveShaper. Based on the proposed system, TBP of a nanosecond-long microwave signal is compressed successfully with a compression factor up to 1.9.

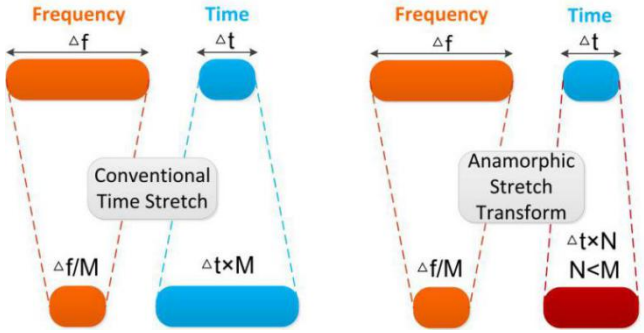

Fig. 1. Comparison of conventional time stretch and AST. The TBP remains constant in conventional time stretch. While in AST, the TBP can be compressed since the bandwidth is reduced without a proportional expansion in temporal duration.

2. Principle

TBP compression for different signals requires different types of group delay [24]. For an input signal having fast variations in the central region of spectrum (as shown in Fig. 2(a) and 2(b)), a sub-linear group delay is desired. The simulation results of linear group delay (green lines) are shown in Fig. 2(c)(e)(g), while the results of sub-linear group delay (blue lines) are illustrated in Fig. 2(d)(f)(h) for comparison. The output signal after linear group delay reflects the spectrum of input signal (see Fig. 2(b) and 2(e)). If a sub-linear group delay is employed, the temporal width of output signal will be compressed (see Fig. 2(e) and 2(f)). Figure 2(g) and 2(h) illustrate the corresponding short-time Fourier transforms, in which the dash boxes mark the temporal width and bandwidth with power density 20 dB less than the peak value. Compared with conventional time stretch, the temporal duration after sub-linear group delay is compressed, while the output bandwidth remains almost unchanged. That means the recording length of the output signal is decreased without increasing the sampling rate. This makes a more efficient use of the available samples. In terms of signals having slow variations in the central region and fast variations in the wings of the spectrum, a super-linear group delay with lower dispersion at the center of the bandwidth is needed (see Fig. 3(d)). In this case, the output temporal duration remains almost constant, while the bandwidth is decreased, smaller than the linear dispersion (see Fig. 3(g) and 3(h)). This means the output signal of the AST could be sampled with lower sampling rate, without increasing the recording time. Compared to the conventional time stretch with linear dispersion, the TBP of AST profile is compressed, leading to a more efficient and easier sampling. Since most signals in practice have spectra like Fig. 2(b), the spectrum of input RF signal in our experiment is feature-dense in the central region and sparse in the wings. Thus a sub-linear group delay should be provided by the dispersive line.

Optics EXPRESS

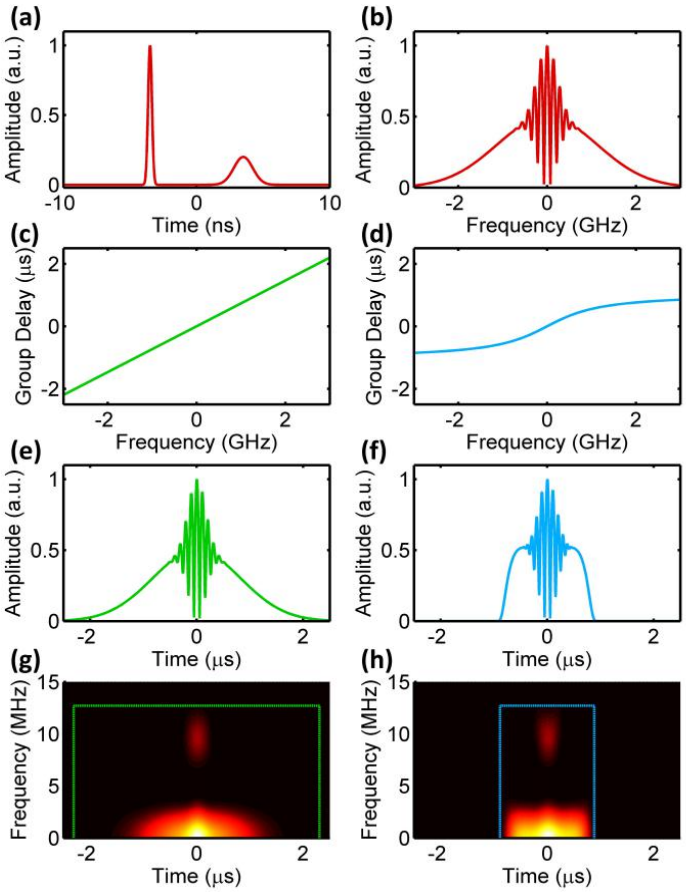

Fig. 2. (a) The waveform of input RF signal. (b) The spectrum of input RF signal. (c) If a linear group delay is used to stretch the input signal, (e) the output signal is a linear scaled version of the input spectrum. (d) If a sub-linear group delay is used to stretch the input signal, the high-frequency parts of the input signal will be stretched less than baseband parts, resulting in a nonlinear frequency-to-time mapping (f). The short-time Fourier transform shows the temporal duration and bandwidth of signals after the linear dispersion (g) and nonlinear dispersion (h). The temporal duration and bandwidth are marked with green dash box (for linear dispersion) and blue dash box (for AST), with power density 20 dB less than the peak value.

Conventional photonic dispersive lines based on optical fiber or fiber Bragg grating (see Fig. 4(a)) usually offer limited amount of dispersion, (e.g. the dispersion value provided by a 100-km long single mode fiber (SMF) is about 1.36×10^{-2} ns/GHz, which is much smaller than the dispersion required for processing nanosecond-long microwave signals. Recently, dispersive lines with ultra-high dispersion amount for microwave signals (see Fig. 4(b)) have been proposed based on a TSC system [23]. It is implemented by temporal modulating an incoherent light source with chirped spectrum. After a suitable length of dispersive medium, the output intensity is proportional to the convolution between the light source spectrum and the temporal intensity of input signals. A microwave dispersion value more than 1ns/GHz can be easily achieved using this method.

Optics EXPRESS

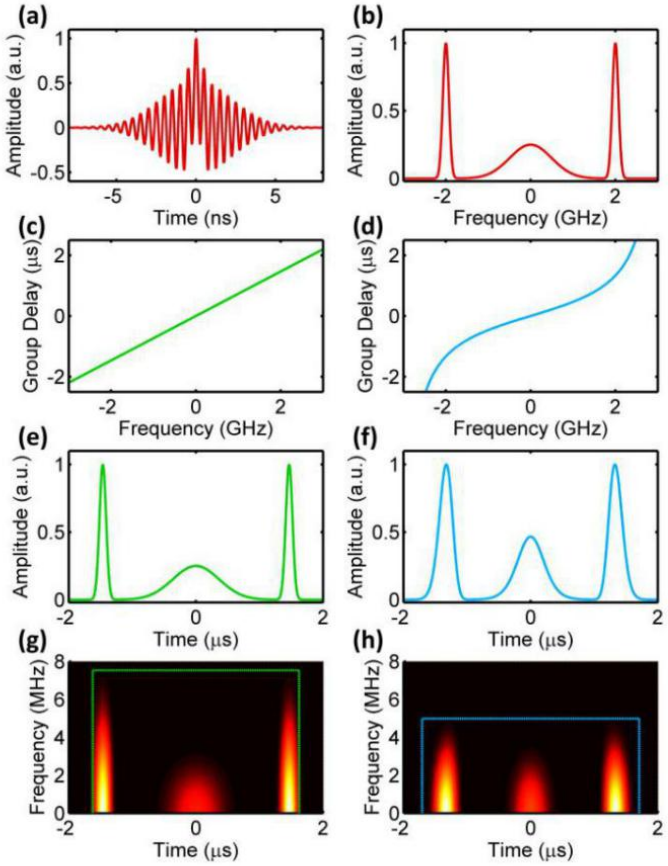

Fig. 3. (a) The waveform of input RF signal. (b) The spectrum of input RF signal. (c) If a linear group delay is used to stretch the input signal, (e) the output signal is a linear scaled version of the input spectrum. (d) If a super-linear group delay is used to stretch the input signal, the low-frequency parts of the input signal will be stretched less than peripheral parts, resulting in a nonlinear frequency-to-time mapping (f). The short-time Fourier transform shows the temporal duration and bandwidth of signals after the linear dispersion (g) and nonlinear dispersion (h). The temporal duration and bandwidth are marked with green dash box (for linear dispersion) and blue dash box (for AST), with power density 20 dB less than the peak value.

Based on the method proposed in [23], the output temporal intensity profile is given by

$$I_{out}(t) = I_{mw}(t) \otimes S(\omega)\Big|_{\omega = t/D_0}. \tag{1}$$

In Eq. (1), $I_{mw}(t)$ is the temporal intensity profile of the input RF signal, $S(\omega)$ represents the spectrum of the incoherent light, $\omega = t / D_0$ denotes the frequency-to-time mapping law determined by the optical dispersive medium, in which D_0 is the dispersion of the optical dispersive medium. To realize a linear dispersion for input microwave signals, $S(t)$ is supposed to have a quadratic phase. However, in practice, the spectrum of the incoherent light is a real function. Thus, the spectrum can be expressed as a sinusoidal variation:

$$S(t) = [1 + \cos(\frac{B_0 \omega^2}{2})]\Big|_{\omega = t/D_0} = 1 + \cos(\frac{B_0 t^2}{2D_0^2}). \tag{2}$$

Optics EXPRESS

As such, the envelope of the output intensity is equivalent to the dispersed input RF signal. The effective dispersion is given by

$$D_{mw} = \frac{D_0^2}{B_0}. \tag{3}$$

By properly choosing a small B_0, D_{mw} can be much larger than D_0. Therefore, an ultra-high linear dispersion for microwave signal can is achieved. As shown in Eq. (2), the frequency-to-time mapping of $S(t)$ is given by

$$\omega(t) = \frac{B_0 t}{D_0^2}, \tag{4}$$

which is a linear function. To realize a sub-linear group delay, we have to find a function to describe the nonlinear frequency-to-time mapping. Tangent function provides a simple but feasible approach for this problem. It has been widely used in the AST of optical signals [20]. So $\omega(t)$ can be written as

$$\omega(t) = C_1 \tan(C_2 t), \tag{5}$$

where C_1 and C_2 are arbitrary real numbers. And as such, $S(t)$ is given by

$$S(t) = 1 + \cos(It\{C_1 \tan(C_2 t)\}) = 1 + \cos[\frac{C_1}{C_2} ln \cos(C_2 t)], \tag{6}$$

where It{} denotes temporal integration operation. If we use the same optical dispersive line where $\omega = t / D_0$. The spectrum of the incoherent light $S(\omega)$ is given by

$$S(\omega) = 1 + \cos[\frac{C_1}{C_2} ln \cos(C_2 D_0 \omega)]. \tag{7}$$

To make sure the frequency-to-time mapping law in Eqs. (4) and (5) are similar in the central part, the following condition needs to be satisfied

$$C_1 C_2 = \frac{B_0}{D_0^2} = \frac{1}{D_{mw}}. \tag{8}$$

Therefore, the group delays supported by Eqs. (2) and (6) are the same in the law frequency area. While in the high frequency part, the group delay supported by Eq. (2) is larger than that supported by Eq. (6). In particular, the value of C_2 is related to the TBP compression factor, which will be discussed later.

Optics EXPRESS

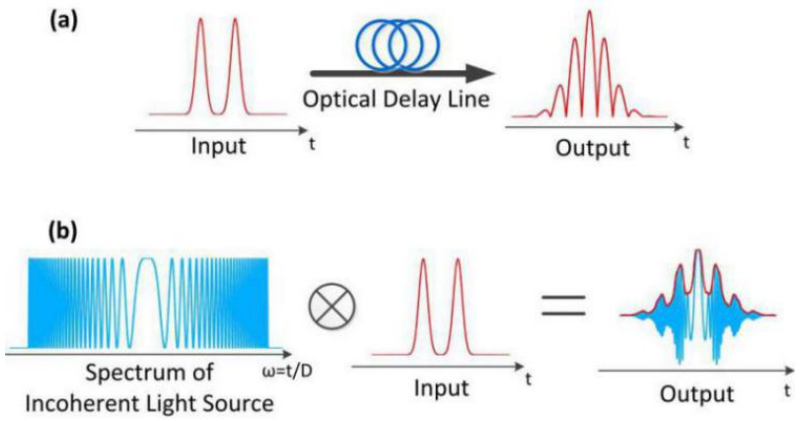

Fig. 4. The comparison of a conventional photonic dispersive line (a) and a microwave dispersive line with ultra-high dispersion value (b). ⊗ represents the convolution operation.

3. Experiment

The experimental setup of our TBP compression system is shown in Fig. 5. The broadband incoherent light is generated by a superluminescent diode (Covega SLD-6716-11748.5.A02) followed by a semiconductor optical amplifier (SOA, Covega BOA-3876) [25]. Then the light is specially filtered by a WaveShaper (Finisar 4000S) with an engineered profile. A RF signal generated from an arbitrary waveform generation (AWG, Tektronix 7122B) is modulated on the filtered incoherent light using an intensity modulator. The optical dispersive medium employed in this system is a section of dispersion compensating fiber (DFC) with a dispersion value of −1314 ps/nm. After amplified by an EDFA, the output optical signal is detected by a 45-GHz photodiode (PD) and monitored in an oscilloscope (Tektronix CSA 8200).

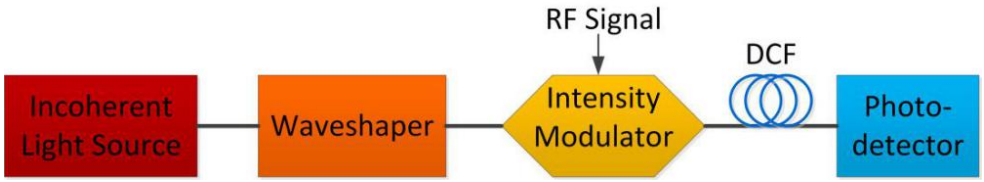

Fig. 5. The experimental setup of the TBP compression system for microwave signals. DCF: dispersion compensating fiber.

By programming the WaveShaper, we can realize linear dispersion or nonlinear dispersion for microwave signals. The measured and simulated spectra of the shaped incoherent light source are shown in Fig. 6. Figure 6(a) represents the shaped spectrum for linear dispersion, where the chirp rate B_0 is chosen to be $2.4\times10^{-6} ns^2/rad$. According to Eq. (3), the effective dispersion for microwave signals D_{mw} is calculated to be $1.17 ns^2/rad$, which enables our scheme to work on GHz-bandwidth microwave signals. Figure 6(b) and 6(c) denote the spectra required for AST with $C_2 = 5\times10^7 rad/s$ and $10\times10^7 rad/s$, respectively. And another parameter C_1 is determined based on Eq. (8). The corresponding group delay profiles are shown in Fig. 7. As can be seen, the group delay profiles of AST have lower dispersion in the wings of the bandwidth, leading to the sides of the spectrum stretched less than the central part. This is desirable as the spectrum of our input signal do not have fast oscillations in the wings, so there is no need to stretch them as much as the central region. In this way, the TBP of microwave signals can be compressed. Meanwhile, group delay profiles of the AST system can be easily engineered by adjusting the WaveShaper, showing a great reconfigurability. However, a programmable optical filter doesn't mean that the proposed scheme can work for

Optics EXPRESS

arbitrary input signals. As explained in Principle section, input signals need to have the potential to be compressed. For sub-linear group delay used in our system, input signals having slow variations in the wing of spectrum are desired. Moreover, the signal will have greater potential to be compressed if the spectrum has a larger proportion of slow variation region.

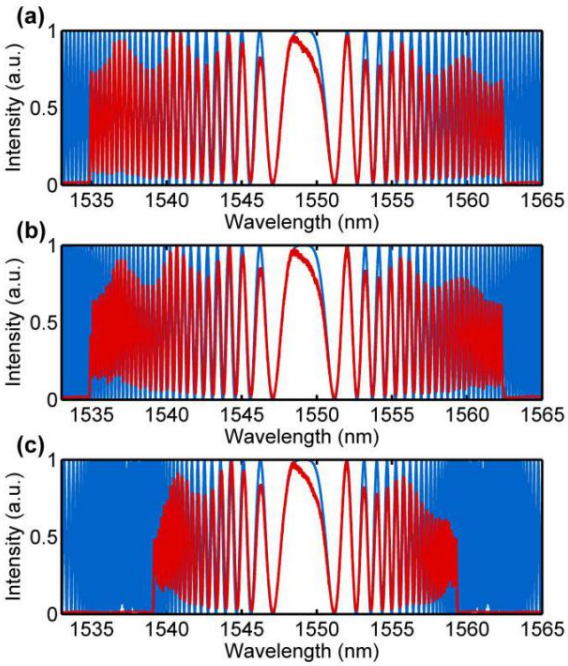

Fig. 6. The measured (red) and simulated (blue)spectra of the incoherent light after a WaveShaper: (a) Linear dispersion, (b) and (c) AST with $C_2 = 5 \times 10^7$rad/s, and $C_2 = 10 \times 10^7$rad/s respectively.

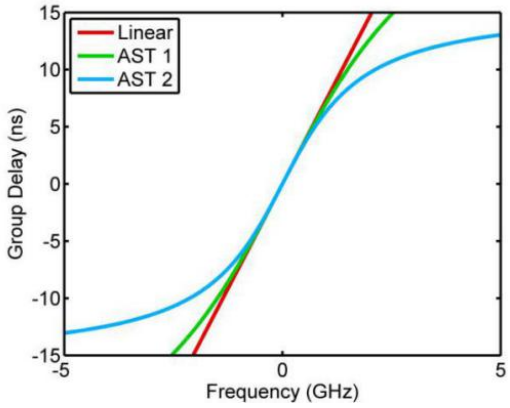

Fig. 7. The corresponding group delay profiles of the linear and AST cases.

The input RF signal and its spectrum are shown in Fig. 8(a) and Fig. 8(b). The input RF signal is a double waveform with different pulse widths. As be seen, the input spectrum has relatively slow oscillations at the sides of bandwidth. In the linear case, i.e. the input optical power spectrum is encoded with a linearly chirped envelope profile by the WaveShaper, and

Optics EXPRESS

the envelope of the output signal is a linear scaled version of the input RF spectrum, as shown in Fig. 9(a). The blue line shows the measured output waveform, while the green line represents the numerically calculated output envelope of the measured input signal in Fig. 8(a). As shown in Fig. 9(a), the time duration of simulation output signal is 50 ns, while the duration of measured waveform is less than 40 ns. The missing information is caused by the bandwidth limitation of our microwave dispersion system. However, in the central region, the measured signal envelope mainly agrees with the simulation one. Thus we have reason to believe that the measured waveform would have the same time duration with the simulation signal if a larger operation bandwidth is provided.

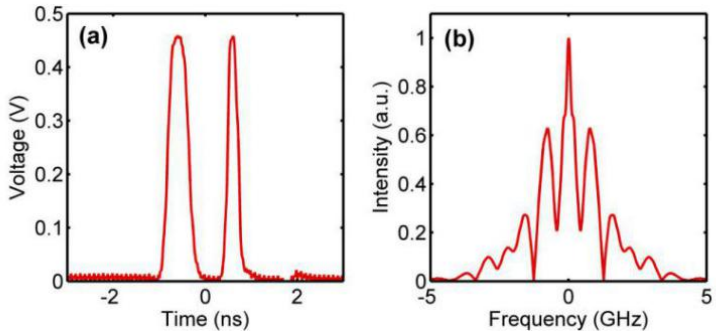

Fig. 8. The waveform (a) and spectrum (b) of input RF signal.

Figure 9(b) and 9(c) show the output waveforms of AST with different value of C_2. Again, there is a good agreement between the simulation (green) and the envelope of measured waveform (blue). However, we can still find some discrepancy, which mainly results from the ASE noise and the spectral unflatness of the broadband source and amplifier. Compared with the linear case, the wings of the output waveform of AST are stretched less than the central region, which leads to a shorter time duration (36ns and 24ns respectively). In order to compare the TBPs of the linear dispersion and AST, the short-time Fourier transform (STFT) of linear dispersion (Fig. 9(e)) and AST (Fig. 9(f) and 9(g)) are calculated. The region of the STFT with power density 20 dB less than the maximum power density is marked by a blue dash line. The green dash box shows the time duration and the bandwidth of output envelopes. As observed, the output bandwidth of AST1 (3.6 GHz) remains almost unchanged, compared to the output bandwidth of linear dispersion, while the temporal duration is squeezed (from 50 ns of linear profile to 36 ns). When a larger nonlinear factor C_2 is employed, the time duration of output envelope will be compressed further, reaching 24 ns. However, the output bandwidth is expanded slightly to 4 GHz, compared to the linear dispersion. This is because the wing part of the output signal is stretched much less than the central part under a larger C_2. In this case, the side part of output waveform has more fast variations than the central part, creating some new high-frequency components. The TBP of output envelopes in the three cases can be easily calculated as 180, 130 and 96 respectively. As can be seen, the TBP of output envelopes in AST 1 and AST 2 are compressed compared with the linear dispersion, with compression factors of 1.4 and 1.9 respectively.

By employing nonlinear dispersion, the recording time can be reduced under the same sampling rate, offering a more efficient way to sample, digitize and store high-speed microwave signals. However, when a larger nonlinear factor is employed, the output envelope bandwidth may increase, requiring a higher sampling rate. To avoid the increasing of sampling rate, the nonlinear factor of AST need to be controlled within a reasonable range. For a given input signal, the nonlinear group delay should be designed to compress the output temporal width as much as possible, without increasing the output bandwidth.

Optics EXPRESS

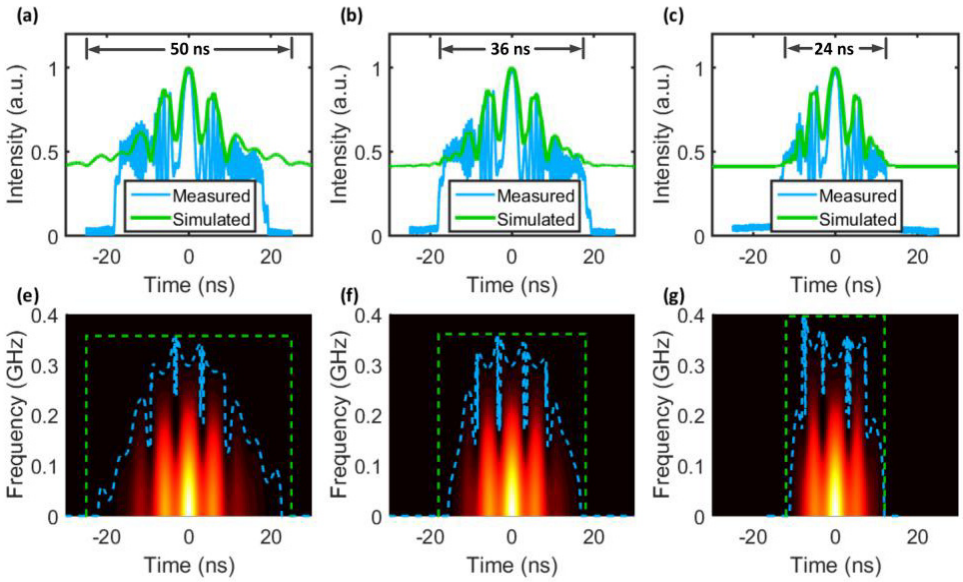

Fig. 9. (a)-(c) Measured output signal (blue line) in case of linear system and AST system with $C_2 = 5 \times 10^7$rad/s, and $C_2 = 10 \times 10^7$rad/s. Green lines are simulated output envelope based on the measured input signal. (e-g) show the STFT of the output envelopes. The region of the STFT with power density 20 dB less than the peak power density is contoured by a blue dash line. The bandwidth and time duration are marked by a green dash box. The time duration of the output envelope is defined as the temporal range up to the fifth notch.

4. Conclusion

We proposed and demonstrated a reconfigurable AST system for GHz-bandwidth microwave signals based on an ultra-high nonlinear dispersion line. The ultrahigh dispersion is induced by using a spectrally shaped incoherent light source followed by a section optical dispersion medium. By using AST technique, the recording time of output envelope can be reduced without increasing the sampling rate. But when the nonlinear factor of group delay increases further, the output envelope bandwidth may be larger than that of linear dispersion. Thus the nonlinear factor of AST need to be controlled within a reasonable range. The TBP of the microwave signal is compressed, with a compression factor up to 1.9 compared with the TBP of linear dispersion. The proposed scheme can provide a more efficient way to sample, digitize and store high-speed microwave signals. By programming the WaveShaper, group delay profiles of the system can be tailored flexibly, opening the path for realization various critical instruments for measurement, generation and processing of high-speed microwave signals in a very simple and practical fashion.

Funding

National Natural Science Foundation of China (61377002, 61321063, 61535012, 61090391 and 61522509).